ChemComm

Novel Cyclopentyl Methyl Ether Electrolyte Solvent with Unique Solvation Structure for Subzero (-40℃) Lithium-ion Battery

Journal:	*ChemComm*
Manuscript ID	CC-COM-01-2022-000188.R2
Article Type:	Communication

COMMUNICATION

Novel Cyclopentyl Methyl Ether Electrolyte Solvent with Unique Solvation Structure for Subzero (-40℃) Lithium-ion Battery

Hari Vignesh Ramasamy, Soohwan Kim, Ethan Adams, Harsha Rao, and Vilas G. Pol*

Received 00th January 20xx,
Accepted 00th January 20xx

DOI: 10.1039/x0xx00000x

1M LiFSI in Cyclopentyl methyl ether is shown as novel electrolyte with unique solvation structure to form a thin robust multilayer solid electrolyte interface with inorganic LiF rich inner layer. Aggregates and Contact Ion Pairs are actively formed in solvation shell and reduced on the graphite anode during lithiation. This EC free electrolyte provides 86.85% initial efficiency, 356 mAh g^{-1} over 350 cycles with an excellent capacity retention of 84 % at 1C rate. An excellent low temperature performance of 370 mAh g^{-1}, 337 mAh g^{-1} and 330 mAh g^{-1} at 0℃, -10℃ and -20℃ at 0.1C rate is recorded. Furthermore at -40℃, the graphite half-cell has a capacity of 274 mAh g^{-1} without electrolyte freezing.

Lithium-ion batteries (LIBs) has a huge market share due to its high energy density, light weight, long cyclability and zero memory effect.[1,2] The state-of-the-art LIB is made of layered oxide cathode, graphite anode and carbonate-based electrolytes. The widespread application of LIBs exposes them to ultralow temperatures below 0℃ in applications like electric vehicles (EV), unmanned aerial vehicles (UAV), submarines, space stations, etc., where they fail to deliver the required capacity.[3] Further the requirement of fast charging batteries that could reach 80% capacity in 15 minutes as per USABC are the major advancements needed in the development of next generation of LIBs. [4] The role of electrolyte plays an important role in the development of better LIBs as it dictates bulk electrolyte conductivity and the formation of the SEI layer.[5] In the electrolyte, the Li^+ ions are surrounded by solvent molecules forming a solvation structure. When these solvated Li^+ ions reach the graphite surface, they strip of their solvation sheath before intercalating into the anode layers. The quicker the desolvation process, the better is its charge transfer kinetics at low temperature and high current rates.[6] Simultaneously, the solvent molecules are reduced on the surface and forms an insulating Solid Electrolyte Interface (SEI) layer. This Li^+ desolvation and migration at the anode electrolyte interface remains the main bottleneck in achieving improved low temperature performance. So far, majority of the electrolyte related works are focused on improving the physical properties of the SEI layer by adding smaller quantity of additives and cosolvents, and thereby improving overall electrochemical properties.[7] The conventional carbonate electrolytes mainly consisted of 1M $LiPF_6$ salt dissolved in highly polar solvents like EC (Ethylene Carbonate), PC (Propylene Carbonate), DEC (Diethyl Carbonate), etc. The salt gets dissociated into Li^+ and PF_6^- and the solvent molecules forms a primary solvation sheath around Li^+ ion. Due to its high polarity, these solvents are tightly bounded to cation and primarily reduced during the initial formation cycles of SEI layer, while the anions remain out of the scene. These ethylene carbonate (EC) derived porous and organic rich SEI layer formed on the graphite surface remains indispensable over ages to prevent solvent co-intercalation and further exfoliation of graphite layers and provides good cyclability at room temperature.[8, 9] This chemistry fails to work at low temperature.

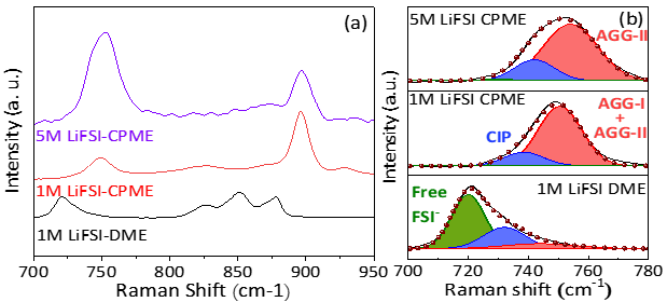

Fig. 1(a) Raman spectra of CE, 1M CPME and 5M CPME, **(b)** Deconvoluted spectra of FSI^- anions in the solvation structure.

To address these issues, several approaches like making binary, ternary, and quaternary solvent mixtures with suitable properties to extend the liquid temperature range [10,11] or by using functional additives [12] to modify the SEI layer has been reported. This could improve the low temperature operation to certain extent. EC being the main culprit freezes even at room temperature making it difficult for low temperature operation.[13] Hence, EC free electrolytes are actively studied in recent days but with less success so far.[14] Recently high concentration electrolytes are being reported as alternative chemistry in which the ratio of the salt is increased with respect to solvent. Thereby, solvent deprivation leads to participation of fluorine containing anions into the solvation structure. In this state, along with solvent molecules contact ion pairs (CIPs) and cation anion aggregates (AGG) prevail.[15a,b] The resulting change in the Fermi level causes reduction of anion species on the anode surface followed by reduction of solvent molecules. This creates a robust LiF rich inorganic SEI layer with superior performance. This technique leads to issues like high cost, high viscosity, inferior wettability, low ionic conductivity, and poor low temperature performance. Zhiang *et al* [16] diluted this high concentration electrolyte using a non-solvating diluent to reduce viscosity and prevent solvent co-intercalation of electrolyte and

H. V. Ramasamy, S. Kim, E. Adams, H. Rao, V. G. Pol.
Davidson School of Chemical Engineering
Purdue University, West Lafayette, IN, 47907, USA.
E-mail: vpol@purdue.edu

studied at -20 ℃. This is a very complex process and could only provide little low temperature improvement. Hence single solvent solution encompassing all required properties is most anticipated. Recently Tan *et al* [17] used isoxazole as a main solvent for graphite anode and able to demonstrate sufficient capacity even at -30 ℃, but still the stability is compromised. Yao *et al* [18a-b] developed 1,4 - Dioxane as weakly solvated electrolyte to modify the SEI layer. But the solubility of this solvent is very low and shows less long-term stability without EC. Hence, screening novel electrolyte solvents could provide the necessary solution.

We report a novel ether-based electrolyte solvent called Cyclopentyl methyl ether (CPME) that shows superior stability and ultralow temperature performance up to -40℃. It has an excellent film forming ability that avoids the need of EC and other high concentration approaches. We demonstrated it by comparing 1M $LiPF_6$ in EC: DEC (1:1) (denoted as Reference) electrolyte with 1M LiFSI in CPME (denoted as 1M CPME hereafter) and 5M LiFSI in CPME (5M CPME) in Li/Graphite coin cells. The CPME derived electrolytes has unique solvation structure that consists of CIPs and AGGs in its solvation shell even in diluted state (1M) as that of high concentrated electrolytes. This CPME solvent has suitable physical properties required for low temperature functioning of LIBs like high boiling point (106℃), ultralow melting point (-140℃), lower dielectric constant and at the same time has high solubility of salt (7M). It is an environmentally safe green solvent commercially available and economically feasible to synthesis. Compared to other ether solvents it does not form peroxide even if exposed to the air atmosphere for several days. It is one of the versatile solvents used in organic chemistry but not yet reported for the battery applications.[19] 1M CPME delivers high capacity of 351 mAh g^{-1} at 1C (372 mAh g^{-1}) and very good stability up to 350 cycles with 84% capacity retention at room temperature. The capacity remains same until -20 ℃ with 100% retention at -20 ℃. Even at -40℃, this electrolyte gives a capacity of 274 mAh g^{-1}. Detailed analysis is carried out using Raman, XPS, and electrochemical methods and the results are summarized below. We performed Raman spectra to visualize the solvation structure of 1M LiFSI in DME, 1M CPME and 5M CPME electrolytes. The intent of using diluted electrolyte of DME is to differentiate the unique solvation structure of diluted CPME electrolyte with that of common ethers. **Fig. 1a** shows the overall spectrum including both anion and solvent molecules. The peaks between 700 cm^{-1} and 775 cm^{-1} belongs to FSI^- anions, whereas the peaks above 800 cm^{-1} denotes DME and CPME solvents, respectively. For 1M LiFSI in DME the peaks at 825, 850 and 875 cm^{-1} denote the free solvent molecules with CH_2 oscillation and C-O stretching behaviour.[16] In 1M and 5M CPME electrolyte the peaks at 820 and 895 cm^{-1} denotes the free CPME solvent molecules.[19] Initial observation of CPME clearly shows that the peak intensity of solvent decreases with increasing salt concentration. In 5M CPME by increasing the salt ratio more solvents are brought inside solvation structure leaving only lesser free solvent molecules. CPME can dissolve very high salt concentration of up to 7 M of LiFSI, which is significantly higher for a weekly solvated electrolyte. The deconvoluted peaks of FSI^- anion is provided in **Figure 1b**. Three different states of FSI^- anion is clearly distinguished using green, purple, and red color corresponding to free FSI^-, contact ion pair (CIP) and Aggregates. [20a] Free FSI^- are those without involving in solvation structure, CIP represents single anion attached to single Li^+ and aggregates denotes single anion attached to two or more Li^+. Diluted DME electrolyte is dominated by free FSI^- anions, which are not available for SEI formation, while the CPME electrolytes has CIP and AGG and its major influence in SEI formation. More peculiar thing of CPME lies in its increased AGG ratio with respect to CIP structures. This is opposed to that of the reported works, in which the CIP dominates. The peak around 750 cm^{-1} for CPME corresponds to two different Aggregate structures. AGG-I represents single FSI^- anion bonded with two Li^+ ion, whereas in AGG-II, FSI^- anion forms bond with three Li^+. Li et al[20b] could achieve similar in their reported Li metal work by using an additional diluting solvent which adds more complexity. Our solvation structure remains unique like that of high concentration salts even in diluted state and first reported for graphite anode.

The electrochemical performance of graphite anode with 1M and 5M

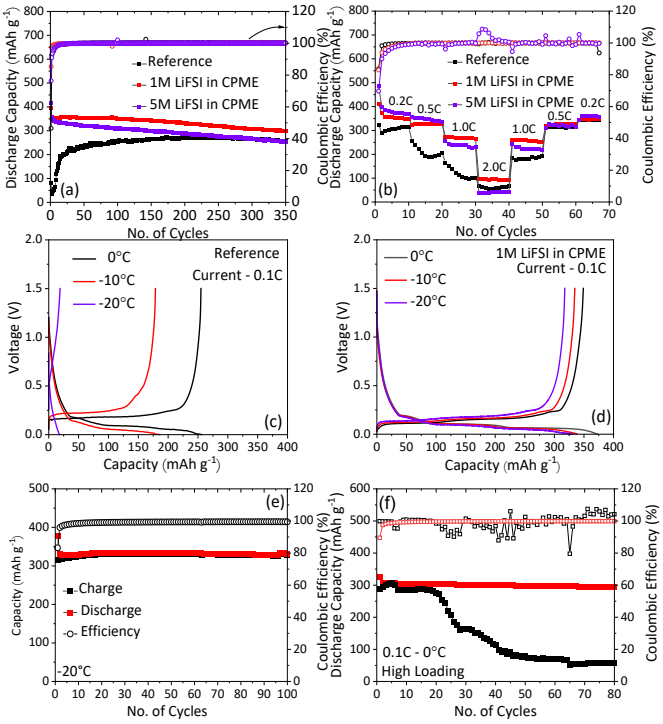

Fig. 2 (a) Cyclability at 1C and **(b)** Rate performance using different electrolytes at 25 ℃. Low temperature performance of graphite electrode in different electrolytes **(c)** Reference electrolyte **(d)** 1M LiFSI in CPME. Low temperature performance of **(e)** low mass loaded electrode at 0.1C rate and **(f)** high active mass loaded graphite electrode

CPME electrolyte is compared with commercial electrolyte in Graphite/Li^+ half-cell and provided in **Fig. 2**. The detailed experimental information is available in **Supporting Information (SI)**. The electrochemical performance is carried out using two different electrode configurations with high (6.2 mg cm^{-2}) and low active mass (1.5 mg cm^{-2}) loading. The discharge capacity-voltage curves obtained at 0.1C for low active mass loading are shown in **Fig. S1**. During initial lithiation of graphite anode, a clear peak appears for CPME electrolytes at 1 V and 1.14 V corresponding to the reduction of electrolytes with anion derived solvation structure on the graphite surface. The absence of this peak in the following cycle gives a clear picture of stable SEI layer formation in the first cycle. This is followed by continuous lithiation of graphite resulting in LiC_6 at the end of discharge.[2] The commercial electrolyte decomposes at a lower voltage of 0.6 V forming a thick SEI layer. Further, the room temperature cyclability of these electrodes is evaluated at 1C (372 mAh g^{-1}) rate up to 350 cycles within 1.5 to 0.001V voltage window (**Fig. 2a**). 1M CPME has a higher first cycle coulombic efficiency of 85.29% higher than the 5M CPME and CE with a value of 76.37 and

46.55 %, respectively. The initial discharge capacity for CE, 1M CPME and 5M CPME are 82 mAh g^{-1}, 395.625 mAh g^{-1} and 416.892 mAh g^{-1}. The reversible capacity obtained from these electrolytes are 82 mAh g-1, 355 mAh g^{-1} and 356 mAh g^{-1}, respectively. After 100 cycles these two electrolytes could still maintain a higher retention of 98.80% and 86.57%. Even after 350 cycles, it has a capacity of 298.72 mAh g^{-1} and 254.675 mAh g^{-1} retaining 84.13% and 71.37% capacity. Throughout cycling the coulombic efficiency remains 100% due to the better compatibility of the electrolyte with graphite anode. The commercial electrolyte starts with a low capacity of 82 mAh g^{-1} and gradually increase with the cycling until it reaches a maximum capacity of 270 mAh g^{-1} and gradually decrease to 256.33 mAh g^{-1} after 350 cycles and starts degrading. This may be due to the formation of unstable and porous SEI layer composed of dominant Li_2CO_3 and small LiF initially and stabilize over cycling.[12] This SEI has electron donating nature and create favourable situation for continuous reduction of electrolytes making capacity degradation over cycling. In contrast 1M CPME forms a robust thin SEI layer made of rich LiF content and small amount of $Li_2C_2O_4$ even at 1C rate. This unique SEI layer with LiF is more favourable for faster Li^+ ion conduction along its grain boundaries, vacancies, defects with reduced charge transfer resistance.[21] 5M LiFSI in CPME forms a slightly thicker LiF rich SEI layer that consumes more Li^+ during initial

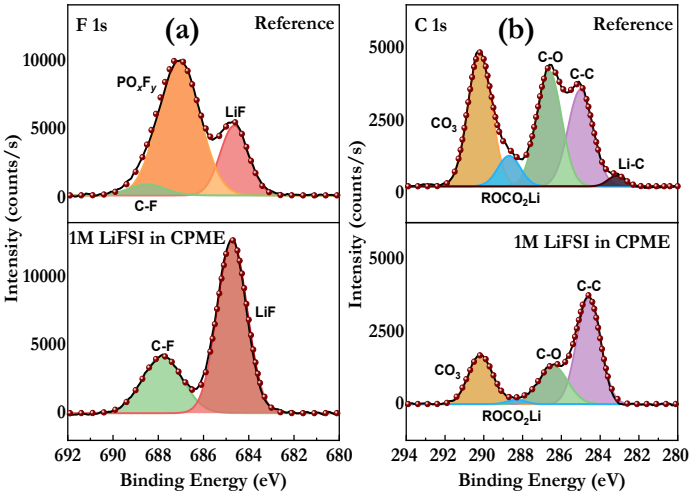

Fig. 3 Deconvoluted XPS spectra of F1s and C1s elements from graphite anode in delithiated state after 10 cycles.

cycle followed by its increased resistance for ion movement. This is evident from the slightly lower capacity retention after prolonged cycling. Overall, these are so far the best cyclability data of graphite anode in a diluted ether electrolyte without any cosolvents, additives and ethylene carbonate. The cycling of these electrolytes at different current rates are provided in **Fig. 2b**. At lower C- rate of 0.2C, the capacity of CPME is similar and higher than commercial one. At higher C-rate 1M CPME has higher capacity of 98.45 mAh g^{-1} due to lower charge transfer resistance and favorable ionic conductivity at the interface. 5M CPME has the lowest capacity of 39.17 mAh g^{-1} due to its higher viscosity and higher charge transfer resistance. By considering the practical feasibility of this electrolyte, we used high areal loading electrodes obtained from Argonne National Laboratory and the results are in **Fig. S2.** The cyclability is tested at 0.5C rate between 0.001 V and 1.5 V till 100 cycles. The initial performance of graphite with CE and CPME has a capacity of 246.68 mAh g^{-1} and 347.05 mAh g^{-1}. First cycle corresponds to formation of SEI layer in CPME electrolyte, whereas CE forms porous organic SEI layer which gets stabilized over cycles as seen from capacity increase to 283.51 mAh g^{-1}. The initial Coulombic efficiency for CPME has a higher value of 86.85 %, the highest reported for an ether-based electrolyte. After 100 cycles, 1M CPME has a highest retention of 91.77%, while CE could only maintain 51.62%. From **Fig. 2c and 2d** 1M CPME electrolyte could deliver highest capacities of 370 mAh g^{-1}, 337 mAh g^{-1} and 331 mAh g^{-1} with respect to 0 ℃, -10 ℃ and -20 ℃ at 0.1C rate between 0.001 to 1.5V. Further at -20 ℃, it retains 100 % of its capacity until 100 cycles at 0.1C rate (**Fig. 2e**). This is by far the highest reported capacity for graphite anode at -20 ℃. Going down to -40 ℃, the electrolyte could still work without freezing and provide a capacity of 273 mAh g^{-1} at 0.005C (**Fig. S3**). The performance of commercial electrolyte-based cell is very poor as it could only retain half the theoretical capacity of 183 mAh g^{-1} at -10 ℃ and almost stopped working with only 20 mAh g^{-1} at -20 ℃. This extraordinary performance at ultralow temperature is due to the very low freezing point (-140 ℃) of the CPME solvent along with the thin, robust, and inorganic LiF rich SEI layer. Similarly, the high loaded electrodes are tested at 0 ℃ using commercial electrolyte and diluted CPME electrolyte at 0.1C rate as shown in **Fig. 2f**. It has a 1st cycle capacity of 289 mAh g^{-1} and 326 mAh g^{-1} and retains 56.9 mAh g^{-1} and 293.24 mAh g^{-1} after 80 cycles with a retention of 20% and 90%. The initial coulombic efficiency is 99.83% for carbonate electrolyte and a very high value of 89.5% for diluted CPME ether electrolyte.

The EIS spectra shown in **Fig. S4** can be divided into four different parts like Ohmic resistance, SEI resistance and charge transfer resistance followed by Warburg diffusion. [22–24] The curves are fitted using equivalent circuit and the resistance values are provided in **insets of Fig. S4e and S4f**. The overall resistance values increase with the decrease in temperature. The Ohmic resistance is seen at high frequency region, where the curve intersects the X axis. This includes the intrinsic properties of the electrolytes and electrodes like conductivity etc. The SEI and charge transfer resistance is provided by the semicircle at the medium frequency region and results from the resistance of the SEI and other interfaces. This value is very much reduced for diluted CPME in the order of 10-fold than commercial one as expected from the robust and thin LiF film formed from the reduction of anion derived unique solvation structure during initial lithiation. LiF SEI layer has improved young's modulus and better stability over cycling. Even though it has poor ionic conductivity, the coexistence of different inorganic and organic species creates defect's, grain boundaries and local charges thereby creating an efficient pathway for ion hopping and migration.[25] This is confirmed by calculating the activation energies at interfaces by using Arrhenius law with respect to various temperatures as shown in **Fig. S4c and S4d.** The diluted CPME has the lower desolvation energy (69.6 kJ mol^{-1}) as compared to that of reference electrolyte (79.39 kJ mol^{-1}) because in this the desolvation is primarily due to dissociation of ion pairs (Li^+ - FSI^-) and aggregates ($3Li^+$ - FSI^-) than Li^+ - solvent molecules. Further Li^+ transport through SEI layer has lower energy for CPME electrolyte due to abundant grain boundaries, defects and hopping sites, while the Li^+ diffusion in porous inorganic SEI of carbonate electrolytes are more energy consuming. Further the Rct and Rsei values obtained from fitting the Nyquist plot using equivalent circuits for reference and diluted CPME at different temperatures are provided in **Fig. S4e and S4f.** The values of CPME are much reduced and negligible in comparison with the commercial electrolyte. XPS analysis is carried out on delithiated graphite electrode after 10 cycles at 0.1C rate in commercial and 1M CPME electrolyte. **Fig. 4** represents the deconvoluted XPS spectra of F1s and C1s elements on

the graphite surface after cycling in reference electrolyte and 1M LiFSI in CPME. The F1s spectra can be divided into 3 different peaks representing C-F (687.7 eV), POxFy (687.06 eV), and LiF (684.58 eV).[12,26,27a] The intensity of POxFy based porous organic specious is higher than the LiF peak in commercial electrolyte resulting from continuous reduction of $LiPF_6$ over cycling. In contrast, the CPME electrolyte has higher content of LiF whereas POxFy peak has been completely disappeared in the spectra. This can be justified as there is no $LiPF_6$ based side reaction in CPME solvent. The predominance of LiF peak is due to the reduction of FSI^- anions from AGG and CIP solvation structures. C-F represents PVDF binder, which has intensity variation due to the thickness of the SEI layer formed.[22] The C1s spectra has four major partitions with CO_3 (290.2 eV), $ROCO_2Li$ (288.6 eV), C-O (286.6 eV), C-C (284.74 eV) respectively. [23,24,27b] The CO_3 represents Li_2CO_3 based solvent derived SEI component, which has been significantly reduced for CPME electrolyte. This is because anions from solvation structure reduce initially on anode surface and forms stable LiF rich SEI layer, preventing further reduction of solvent molecules. $ROCO_2Li$ and C-O corresponds to an organic species available as an outer layer of SEI with LiF as the inner layer. Thickness of the SEI layer formed is inferred from C-C bond intensity of graphite anode. Higher intensity is due to thin SEI layer and vice versa. Finally, we put forward 1M LiFSI in CPME as a novel EC free electrolyte for low temperature and fast charging applications with its unique anion derived SEI layer.

The results provide a new way to achieve the SEI composition without approaching the costly and complex high concentration route. The results are impressive with high capacity of 331 mAh g^{-1} at 0.1C and 100% stability at -20 ℃ and could reach up to -40℃. The bilayer structure of Solid electrolyte interface (Inorganic LiF rich inner core and thin outer organic layer) as confirmed from XPS analysis helps in overcoming the main bottleneck of highest desolvation energy that was taken as a research problem initially.

VP truly thanks the financial support from the Naval Enterprise Partnership Teaming with Universities for National Excellence (NEPTUNE), Office of Naval Research (Grant # N000142112070) and the Program Manager, Maria Medeiros. The provisional US patent (PRF # 2022-POL-69635 and USPTO # xxxxxxxx) is filed by Dr. D. H. R. Sarma, Registered USPTO Patent Practitioner, of the Purdue Research Foundation, IN, USA on the research work displayed in this manuscript.

Conflicts of Interest

"There are no conflicts to declare".

Notes and references

[1] M. Li, J. Lu, Z. Chen, K. Amine, *Advanced Materials* **2018**, *30*, DOI 10.1002/adma.201800561.

[2] J. Xu, X. Wang, N. Yuan, B. Hu, J. Ding, S. Ge, *Journal of Power Sources* **2019**, *430*, 74–79.

[3] A. Gupta, A. Manthiram, *Advanced Energy Materials* **2020**, *10*, DOI 10.1002/aenm.202001972.

[4] M. Weiss, R. Ruess, J. Kasnatscheew, Y. Levartovsky, N. R. Levy, P. Minnmann, L. Stolz, T. Waldmann, M. Wohlfahrt-Mehrens, D. Aurbach, M. Winter, Y. Ein-Eli, J. Janek, *Advanced Energy Materials* **2021**, *11*, DOI 10.1002/aenm.202101126.

[5] K. Xu, *Chemical Reviews* **2014**, *114*, 11503–11618.

[6] Q. Li, D. Lu, J. Zheng, S. Jiao, L. Luo, C. M. Wang, K. Xu, J. G. Zhang, W. Xu, *ACS Applied Materials and Interfaces* **2017**, *9*, 42761–42768.

[7] F. Han, Z. Chang, X. Liu, A. Li, J. Wang, H. Ding, S. Lu, in *Journal of Physics: Conference Series*, IOP Publishing Ltd, **2021**.

[8] N. Ehteshami, L. Ibing, L. Stolz, M. Winter, E. Paillard, *Journal of Power Sources* **2020**, *451*, DOI 10.1016/j.jpowsour.2020.227804.

[9] X. G. Yang, T. Liu, C. Y. Wang, *Nature Energy* **2021**, *6*, 176–185.

[10] Q. Li, S. Jiao, L. Luo, M. S. Ding, J. Zheng, S. S. Cartmell, C. M. Wang, K. Xu, J. G. Zhang, W. Xu, *ACS Applied Materials and Interfaces* **2017**, *9*, 18826–18835.

[11] C. S. Rustomji, Y. Yang, T. K. Kim, J. Mac, Y. J. Kim, E. Caldwell, H. Chung, Y. S. Meng, *Science* **2017**, *356*, DOI 10.1126/science.aal4263.

[12] G. Song, Z. Yi, F. Su, L. Xie, C. Chen, *ACS Applied Materials and Interfaces* **2021**, *13*, 40042–40052.

[13] S. Klein, S. van Wickeren, S. Röser, P. Bärmann, K. Borzutzki, B. Heidrich, M. Börner, M. Winter, T. Placke, J. Kasnatscheew, *Advanced Energy Materials* **2021**, *11*, DOI 10.1002/aenm.202003738.

[14] C. E. L. Foss, A. M. Svensson, Ø. Gullbrekken, S. Sunde, F. Vullum-Bruer, *Journal of Energy Storage* **2018**, *17*, 395–402.

[15] (a)J. Wang, Q. Zheng, M. Fang, S. Ko, Y. Yamada, A. Yamada, *Advanced Science* **2021**, *8*, DOI 10.1002/advs.202101646. (b) J. Zheng, J. A. Lochala, A. Kwok, Z. D. Deng, *Adv. Sci.,* **2017**, 4, 1700032

[16] L. L. Jiang, C. Yan, Y. X. Yao, W. Cai, J. Q. Huang, Q. Zhang, *Angewandte Chemie - International Edition* **2021**, *60*, 3402–3406.

[17] S. Tan, U. N. D. Rodrigo, Z. Shadike, B. Lucht, K. Xu, C. Wang, X. Q. Yang, E. Hu, *ACS Applied Materials and Interfaces* **2021**, DOI 10.1021/acsami.1c05894.

[18] (a) Y. X. Yao, X. Chen, C. Yan, X. Q. Zhang, W. L. Cai, J. Q. Huang, Q. Zhang, *Angewandte Chemie - International Edition* **2021**, *60*, 4090–4097. (b) J. Choi, H. Jeong, J. Jang, A. R. Jeon, I. Kang, M. Kwon, J. Hong, M. Lee, *J. Am. Chem. Soc*., **2021**, 143, 9167-9176.

[19] L. Xing, X. Zheng, M. Schroeder, J. Alvarado, A. V. W. Cresce, K. Xu, Q. Li, W. Li, *Acc. Chem. Res.,* **2018**, 51, 282-289.

[20] (a) X. Cao, H. Jia, W. Xu, J.-G. Zhang, *Journal of The Electrochemical Society* **2021**, *168*, 010522. (b) T. Li, X. Q. Zhang, N. Y. Xing, L. P. Hou, X. Chen, M. Y. Zhou, J. Q. Huang, Q. Zhang, *Angewandte Chemie - International Edition* **2021**, *60*, 22683–22687.

[21] Q. Zhang, J. Pan, P. Lu, Z. Liu, M. W. Verbrugge, B. W. Sheldon, Y. T. Cheng, Y. Qi, X. Xiao, *Nano Letters* **2016**, *16*, 2011–2016.

[22] M. Xu, L. Zhou, L. Hao, L. Xing, W. Li, B. L. Lucht, *Journal of Power Sources* **2011**, *196*, 6794–6801.

[23] R. Guo, Y. Che, G. Lan, J. Lan, J. Li, L. Xing, K. Xu, W. Fan, L. Yu, W. Li, *ACS Applied Materials and Interfaces* **2019**, *11*, 38285–38293.

[24] P. Shi, L. Zhang, H. Xiang, X. Liang, Y. Sun, W. Xu, *ACS Applied Materials and Interfaces* **2018**, *10*, 22201–22209.

[25] J. Tan, J. Matz, P. Dong, J. Shen, M. Ye, *Advanced Energy Materials* **2021**, DOI 10.1002/aenm.202100046.

[26] C. T. Yang, Y. Qi, *Chemistry of Materials* **2021**, *33*, 2814–2823.

[27] (a) Z. Ahmad, V. Venturi, H. Hafiz, V. Viswanathan, *Journal of Physical Chemistry C* **2021**, *125*, 11301–11309. (b) M. C. Smart, B. L. Lucht, S. Dalavi, F. C. Krause, B. v. Ratnakumar, *Journal of The Electrochemical Society* **2012**, *159*, A739–A751.